



University of Novi Sad

DSpace-CRIS Repository

<https://open.uns.ac.rs>

2022-10-26

Monitoring of Drug Release via Intra Body Communication with an Edible Pill

Leonardo Lamanna, Pietro Cataldi, Marco Friuli, Christian Demitri, Mario Caironi

Wiley-VCH

Leonardo Lamanna, Pietro Cataldi, Marco Friuli, Christian Demitri, and Mario Caironi. 2022. Monitoring of Drug Release via Intra Body Communication with an Edible Pill. *Advanced Materials Technologies* 8(1). doi: <https://doi.org/10.1002/admt.202200731>.

<https://open.uns.ac.rs/handle/123456789/32631>

Downloaded from DSpace-CRIS - University of Novi Sad

Monitoring of Drug Release via Intra Body Communication with an Edible Pill

Leonardo Lamanna,* Pietro Cataldi, Marco Friuli, Christian Demitri, and Mario Caironi*


Oral drug administration provides a convenient and patient-compliant way for drug delivery, especially for chronic diseases and prolonged pharmacological treatments. However, due to the repetitiveness of such therapeutic approach, the patients are led to neglect/forget the therapy affecting the healthcare delivery. Indeed, the non-adherence to pharmacological prescriptions and the unknown amount of real-time drug release result in a non-compliant therapeutic drug level over the protracted therapies. The proposed technology will enable the monitoring of both pharmacological adherence and real-time drug release. The approach exploits a passive intrabody communication (IBC) activation in order to enable an edible pill, realized starting from food additives and food-grade materials, to monitor pharmacological adherence. Following activation, the signal is modulated by IBC coupling switching triggered by pill degradation in a gastrointestinal tract, resulting in a monitored drug release. The proof-of-concept is designed for a targeted release and monitoring of Metformin in the intestine. The system shows an *in vitro* limit of cumulative drug release detection of $18 \mu\text{g mL}^{-1}$ and a limit of real-time drug release detection of $2 \mu\text{g mL}^{-1} \text{min}^{-1}$. This platform represents the first solution to monitor passive drug release in real-time, from intake to complete absorption, enabling unique and long-sought healthcare therapy and treatment opportunity.

1. Introduction

The technological healthcare revolution is deemed to transform our lives.^[1,2] The use of wearable,^[3,4] implantable,^[5] and ingestible devices^[6] will deliver continuous monitoring of physiological metrics, personalized therapies, and rapid sharing of data

L. Lamanna, P. Cataldi, M. Caironi
Center for Nano Science and Technology @PoliMi
Istituto Italiano di Tecnologia
Via G. Pascoli, 70/3, Milano 20133, Italy
E-mail: leonardo.lamanna@unisalento.it; mario.caironi@iit.it

L. Lamanna, M. Friuli, C. Demitri
Department of Engineering for Innovation
Campus Ecotekne
University of Salento
Via per Monteroni, Lecce 73100, Italy

 The ORCID identification number(s) for the author(s) of this article can be found under <https://doi.org/10.1002/admt.202200731>.

© 2022 The Authors. Advanced Materials Technologies published by Wiley-VCH GmbH. This is an open access article under the terms of the Creative Commons Attribution License, which permits use, distribution and reproduction in any medium, provided the original work is properly cited.

DOI: 10.1002/admt.202200731

between patients and caregivers, offering new and unprecedented opportunities for diagnosis and treatments. In this context, ingestible electronic (IE) devices represent an emerging key tool supporting medicine.^[6] Such technology easily enthralls our minds, picturing us in the Fantastic Voyage of Isaac Asimov. However, IE was conceived as far back as 1957, when the first pH-endoradiosonde was presented.^[7] IE has by then achieved remarkable performances exploiting the use of standard electronics (e.g., PillCam, IntelliCap),^[8,9] but the bulky design, the use of toxic materials, the necessity of ex-post recollection, and the need of medical supervision pose limitations in the use of such a platform.^[10–12] In fact, risks of retention and obstruction are recorded with a percentage that reaches 13% in patients with Crohn's disease;^[6,13] in the perspective of mass applications, this would require unsustainable resorting to surgery.

More recently, edible electronics have been conceptualized to tackle such issues at the root and to develop environmentally friendly, cost-effective, safe, and self-administrable edible devices.^[14–17] This transformation requires introducing new materials from food and food derivatives, approved by Food and Drug Administration/European Food Safety Authority (FDA/EFSA), into swallowable electrical appliances, enabling a new healthcare platform. One of the most attractive visions and expectations from edible electronics is developing an edible device that is affordable, without ethical issues, and secure for monitoring all the pharmacological therapy in chronic and thorny diseases.

For many pathologies (e.g., diabetes, hypertension, psychiatric illness), precise and sustained pharmacological therapy is crucial for disease control and/or recovery.^[18] Such administrations are obtained by two main approaches: a correct pharmacological adherence^[19–21] and a controlled drug release system.^[22]

Pharmacological adherence describes the degree to which a patient correctly follows a medical prescription. World Health Organization estimated that only $\approx 50\%$ of patients with chronic diseases living in developed countries follow treatment recommendations with meager rates for diabetes, asthma, and hypertension.^[23,24] This oversight translates into an economic cost of 300 B\$ in the United States and 125 B€ in Europe, comprehensive of hospitalizations, complication treatments, and wasted drugs.^[24–27] To improve pharmacological adherence

in chronic therapies, a key role has been assigned to mobile health (mHealth) through messaging and a dedicated reminder mobile app.^[28] Noteworthy, in 2015, Proteus Digital Health Inc. presented the first ingestible CMOS integrated-circuit micro-sensor, designed to be incorporated into every type of tablet, to monitor medication adherence.^[26]

On the other side, controlled drug release systems allow tuning of drug dosages to specific rates. Over the past few decades, drug delivery systems have benefited patient compliance to medications and recovery. As a result, since the first controlled release formulation, approved in the 1950s, drug delivery and release systems have been steadily innovated, as opposed to the research of brand-new drugs, which has been decreasing.^[29] Indeed, He et al.^[30] estimated that drug delivery development cost is only 10% compared to developing a new pharmaceutical. Drug delivery systems aim to enhance the drugs' pharmacological activities, overcoming problems of solubility, aggregation, bioavailability, biodistribution, selectivity, and reducing the side effects.^[22,31–33] Despite all these efforts, drug delivery systems miss real-time drug release monitoring, which is only retroactively evaluated via blood, tissue, and excrement analysis.^[34,35] Such a procedure is expensive and gives only statistical results on drug release in patients who take drugs every day. Indeed, release profiles vary depending on metabolism, alimentation, and proper drug assumption.^[36,37]

A technology able to deliver real-time information on pharmacological adherence and drug release, enabling an instantaneous picture of when, where, and how much drug was released, would be disruptive.

Edible electronics have the potential to offer a solution, but concrete demonstrations are scarce. One of the main bottlenecks in developing such safe devices is represented by implementing a proper sensing and communication system with edible components. Indeed, standard wireless communication platforms such as Bluetooth, Zigbee, or Wi-Fi require complex CMOS circuits, low impedance conductors for antenna implementation, and relatively high power density (hundreds nJ bit⁻¹), not currently replaceable with edible electronics.^[38,39] In this context, the most promising communication strategy is the Intra Body Communication (IBC) introduced by Zimmerman in 1996.^[40] IBC is a wireless, bioinspired (i.e., from the nervous system) communication platform that exploits the intrinsic ionic conductivity of the body to propagate a signal, generating a so-called wireless body area network (WBAN).^[41,42] In literature, two main coupling techniques are reported for IBC: galvanic and capacitive. The galvanic coupling has four electrodes in contact with the human body, two for transmission and two for reception (Figure S1, Supporting Information).^[41] The capacitive coupling, instead, exploits just two electrodes in contact with the human body: an electrical potential is generated between the signal (in contact) and ground (directed towards the external environment) electrodes of the transmitter and detected by the receiver, which also has a pair of signal and ground electrodes (in the same configuration of the transmitter, Figure S1, Supporting Information). The electric potential induced by the transmitter is coupled to the human body and is detected by the receiver through it, with the advantage that much of the signal is confined to the human body, minimizing the transmission power required.^[41,43] IBC

technology has the advantage of low power consumption (<10 pJ bit⁻¹ for capacitive coupling)^[44] and the possibility to employ high impedance conductors, more easily accessible with the current stage of development of edible electronics.^[14,45]

To date, IBC has been exploited to generate a WBAN connecting different wearable and/or implanted devices.^[46–49] Proteus Digital Health Inc. exploited galvanic IBC in the first FDA-approved ingestible sensor designed to be incorporated into every tablet or capsule, for measuring pharmacological adherence.^[26]

In this work, we propose an approach for the electrical monitoring of passive drug release (hereafter defined as “eDi-MoRe”) through an edible device exploiting the switching between IBC coupling modes. eDi-MoRe consists of a pill made of a conducting composite and an insulating degradable/digestible drug-filled matrix. Each part is connected to one terminal of an AC signal generator. Metformin, which is the preferred first-line oral blood-glucose-lowering agent to manage type 2 diabetes,^[50] has been chosen as the target drug in this study. Indeed, the necessity of a constant drug blood level, the low bioavailability, and short half-life of metformin,^[51,52] together with the prevalence of intestine absorption,^[53] make the necessity for the development of a targeted, controlled, and monitored metformin release system minimizing the daily drug intake and correlated side effects and augmenting patient compliance.

The eDi-MoRe concept has been tested *in vitro* by exploiting simulated gastrointestinal fluids and benchtop AC signal generators mimicking a future edible circuit integrated into the pill.^[54] Upon ingestion, the pill is delivered intact to the intestine protected by an electrically insulating oil layer, sealed in a commercial gastro-resistant capsule, which prevents both signal transmission and drug release. Once the pill reaches the intestine, the environmental/pH change triggers the activation of the eDi-MoRe device, by the dissolution of the external gastro-resistant capsule. The conductive part of the pill comes into contact with the intestinal fluid, and an IBC capacitive coupled signal is transmitted, allowing to determine the time elapsed from ingestion of the pill to its entrance into the intestine, corresponding to the start of drug release. The drug-filled composite has been engineered to dissolve in simulated intestinal fluids (SIF). This dissolution leads to a gradual switching between capacitive to galvanic coupling with a consequent reduction in the signal transmission amplitude and to a controlled drug release. The transmitted signal reaches its minimum by the complete pill dissolution, which partially “short-circuits” the AC signal, switching to a galvanic IBC coupling. This platform could pave the way for a widespread technology for the remote monitoring of passive drug delivery, providing simultaneous pharmacological adherence and real-time drug release information.

2. Results and Discussion

The eDi-MoRe concept is presented in **Figure 1a,b**. The eDi-MoRe device is designed to pass through the stomach intact (Figure 1a) and reach the intestine where metformin is primarily absorbed. As such, a gastro-resistant and electrically insulating shell is necessary. Such design guarantees that the capacitive coupled IBC signal transmission starts only in the intestine along

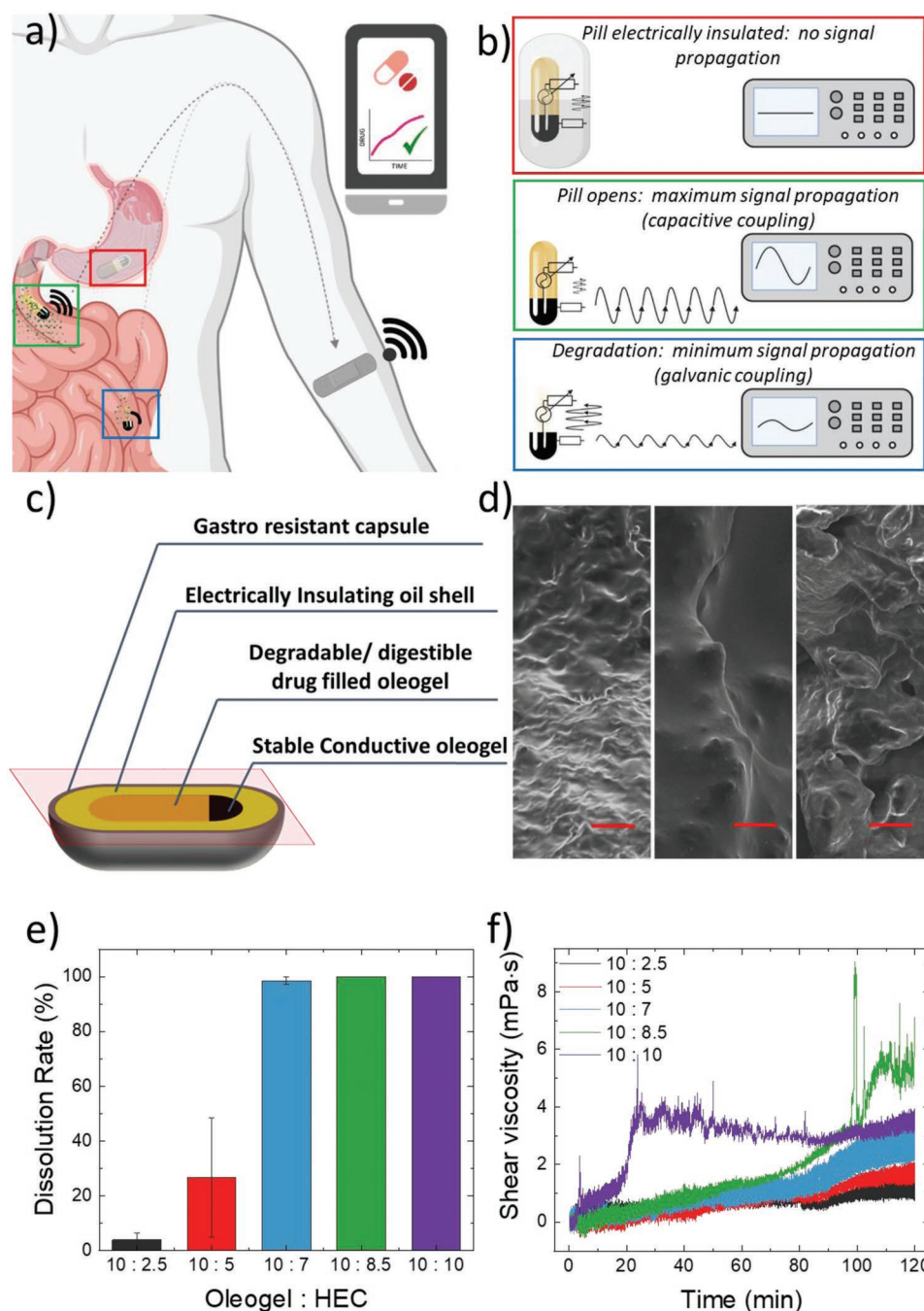


Figure 1. a) Representation of the general concept of IBC activation in the intestine, its modulation, and time-controlled drug release; b) Scheme of device activation and switching from capacitive to galvanic coupling; c) Cross-section of the Proof of Concept device; d) from left to right: SEM image of pure wax-oil oleogel, 10:2.5 and 10:10 oleogel matrix to hydroxyethylcellulose (HEC) ratio (scale bar 40 μm); e) Dissolution rate of the degradable drug-filled oleogel part of the pill in SIF after 120 min; f) Real-time measurement of viscosity change of the pills in SIF due to the different ratio of HEC in the pill formulation.

with the drug release, upon dissolution of the protective gastro-resistant shell (Figure 1b). After such passive activation, the read-out signal amplitude is attenuated along the intestinal tract, again according to a passive mechanism, by the gradual dissolution of the degradable insulating metformin-filled part. Such dissolution gradually releases the drug, and the release can be monitored by signal attenuation. The signal transmission reaches its minimum by the complete pill dissolution,

which partially short-circuits the AC signal (galvanic coupling) (Figure 1b).

2.1. eDi-MoRe Materials

The structure of the eDi-MoRe device is schematized in Figure 1c and it has been developed starting from food-grade

materials. The external protective shell is composed of a commercially available gastro-resistant capsule filled with electrically insulating sunflower oil that seals the core of the pill. The stable edible conductive part has been presented in our previous work.^[55] Briefly, the conductive oleogel (resistivity $\approx 100 \Omega \text{ cm}^{-1}$), constituted by beeswax (E 901) and sunflower oil with the weight ratio of 25:75 and loaded with 40 wt% of Activated Carbon (E153), has been employed. An insulating oleogel matrix made with the same components, without the activated carbon, has been used as a degradable/digestible matrix for drug encapsulation. The easy processability and the low dielectric constant of sunflower oil and beeswax (≈ 3 ^[56] and ≈ 2 ,^[57] respectively), allow the realization of the insulating scaffold. This part of the device has been engineered to trigger the shift between capacitive and galvanic IBC coupling and, simultaneously, enable the drug release. The device preparation is described in the materials and method section and graphically described in Figure S2 (Supporting Information); a real device picture is reported in Figure S3 (Supporting Information).

The insulating oleogel is loaded with 10 wt% of metformin. In this system, hydrophobic drugs can not be tested, since they will be entrapped in the oleogel for a long time after the matrix disintegration.^[58–59] The increase in the oil content does not affect the pill dissolution at body temperature (37 °C). Indeed, the oleogel starts to disintegrate above 60 °C in stirring water as shown in Supplementary Figures S4a,b (Supporting Information). Note that the conductive oleogel is stable up to 90 °C, as shown in Figure S4c (Supporting Information).

Hydroxyethylcellulose (HEC – E1525) has been added as a filler in the insulating oleogel to trigger the pill disintegration in the intestine. HEC is a hydrophilic natural polysaccharide, exploited in cosmetics,^[60] hydrogel manufacturing,^[61] encapsulant,^[62] and drug hydrophilization elements.^[63–64] Other materials such as sucrose and chitosan have been preliminarily tested, with unsuccessful results (Figure S5, Supporting Information). Different amounts of HEC have been added to tune the disintegration time and drug release rate (from 10:2.5 to 10:10 in terms of oleogel:HEC ratio, hereafter defined as samples 10:2.5, 10:5, 10:7, 10:8.5, and 10:10). Microscopically, SEM images show a correlation between the increase of the HEC content and the increase of the material roughness and porosity (Figure 1d, full pictures are reported in Figure S6, Supporting Information). The roughness increase leads to an increase in the surface area in contact with fluids. As such, the HEC in contact with the solution increase, enhancing the water absorption of the composite, as confirmed by the contact angle measurement (Figure S7, Supporting Information). The dissolution rates have been tested in SIF at 37 °C (details in Materials and Methods). The samples 10:2.5 and 10:5 were not completely dissolved after 120 min. In particular, 10:2.5 and 10:5 samples show a partial dissolution of $\approx 5\%$ and $\approx 30\%$, respectively (Figure 1e). On the other hand, the samples with higher HEC content dissolved completely in SIF after 120 min. Noteworthy, the sample 10:10 shows a complete disintegration after 20 min (Figure 1f), with an abrupt viscosity increase caused by particulate presence in the solution (Figure S8, Supporting Information). All the other samples show a homogenous erosion rate, as shown in Figure 1f, where the shear viscosity increases homogeneously with time.

2.2. Electrical Characterization

In eDi-MoRe device, along with the degradation and drug release, a gradual read-out signal attenuation, corresponding to a gradual switching between the capacitive and galvanic coupling of the IBC, takes place (Figure 1a,b). IBC based on capacitive coupling has lower signal attenuation with respect to galvanic coupling. Indeed, galvanic IBC has a primary signal path between the transmission electrodes, and only a small secondary current goes through the receiver^[41] (Figure S1, Supporting Information). As a result, with galvanic coupling, the body partially short-circuits the transmission signal, leading to a higher signal transmission attenuation. On the contrary, capacitive IBC has a primary signal path through the human body, and just a small part of this signal is lost towards the external ground (secondary path).^[41]

In order to simulate the IBC switching mechanism in the human body (Figure 1a,b), *in vitro* experiments have been performed, using a tank of 64L, filled with simulated gastrointestinal fluids or physiological saline solution, to mimic the ionic conductivity in the human body^[65,66] (Figure S9, Supporting Information). As discussed above, an IBC channel is available only upon dissolution of the gastro-protective capsule in SIF, exposing the edible electrode to the human body fluids and allowing a signal transmission through capacitive coupling. Preliminarily, the resistance to the gastric environment and the electrical insulation of the pill has been verified using Simulated Gastric Fluids (SGF), followed by verification of the activation in SIF (Figure S10, Supporting Information). Experiments confirmed that the proposed pill shell prevents both the electrical signal propagation and the drug release in SGF for more than 40 min. Indeed, the impedance between the edible conductor and the receiver remains constant (Figure S10, Supporting Information). This ensures the delivery of eDi-MoRe device intact to the intestine, where the metformin has to be absorbed. The gastro-protective shell is dissolved after ≈ 10 min in SIF (Figure S10, Supporting Information).

The capacitive IBC channel has been characterized using stable devices (without HEC) exploiting the same setup presented in Figure S9 (Supporting Information). In particular, the impedance between the conductive oleogel and the receiver has been characterized (see details of Impedance analysis in Experimental Section) for different pill dimensions and at different distances, ranging from 10–50 cm, representative of the IBC signal transmission in the body. The impedance variation is negligible in both cases (Figures S11 and S12, Supporting Information), as reported in previous studies for the capacitive IBC.^[67,68] In human IBC, the higher impedance tissue is represented by the skin, a fatty and poor hydrated tissue containing dead cells.^[69,70] In order to model this impedance in the system, an *ex vivo* pork rind has been used as an interface,^[71,72] and a commercial adhesive electrode has been placed on it as a receiver (self-adhering Tesmed electrodes $4 \times 4 \text{ cm}^{-2}$). The experiment of whole *ex vivo* animals is excluded since such animals are deprived of liquid components (e.g. gastrointestinal fluid and blood). The results show a slight impedance increase, compared to the receiver immersed in the tank, quantifiable with an in-series resistance of $\approx 200 \Omega$ (data and details in Figure S13, Supporting Information).

Then, the degradable (i.e., filled with HEC) eDi-MoRe device has been characterized. The impedance and the electrical signals are measured with the setup shown in Figure S9 (Supporting Information). In light of the results reported above, such a setup was simplified using a 1 L beaker filled with different simulated solutions held at 37 °C, a temperature that lets us mimic the condition of the in vivo body environment.

We have first characterized the impedance between the electrode in the pill in contact with the digestible/degradable drug-filled composites and the receiver as a function of the dissolution time in SIF (details in Impedance analysis of Experimental Section). The modulus and phase of the impedance for the sample 10:7 are reported in Figure 2a,b. The impedance data

of all the other samples are reported in Figure S14 (Supporting Information). The material dissolution, the rate of which is plotted in Figure 1e, leads to an overall impedance reduction for all the samples. In particular, at time 0, all the systems show a pure capacitive behavior that, with time, is transformed into a constant phase element by the material hydration and dissolution discussed in Figure 1 and then in a mostly resistive behavior. Sample 10:5 (Figures S14a,b, Supporting Information) shows a constant impedance for 60 min, which slightly decreases until 160 min. In this sample, just the outer part of the pill is hydrated/dissolved. Indeed, sample 10:5 showed just a partial dissolution ($\approx 30\%$), as shown in Figure 1e. All the other samples, which have shown a complete dissolution,

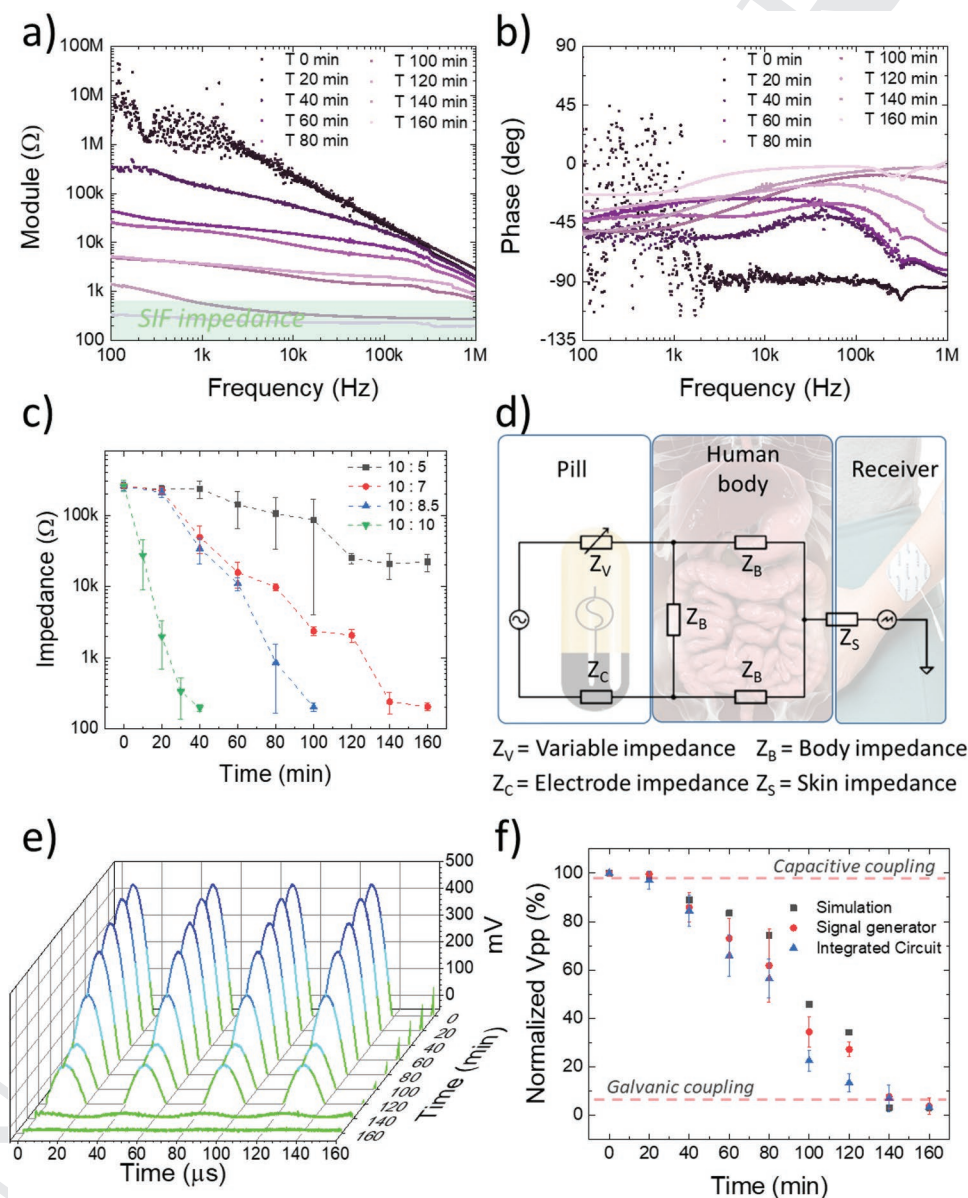


Figure 2. a,b) Module and Phase of the impedance measured during the dissolution of the device with ratio of oleogel matrix:HEC of 10:7. c) Impedance measured at 10 kHz during the eDi-MoRe device dissolution in SIF. d) Equivalent circuit model of the IBC passive modulation; e) Passive IBC modulation due to the insulating degradable/digestible drug-filled matrix dissolution for the sample 10:7. f) Normalized peak-peak signals for the IBC passive modulation obtained with a signal generator, integrated circuit (IC), and simulation.

lead to a substantial impedance decrease, until only the SIF impedance is measured, indicating that the electrode is completely exposed to the SIF solution; this condition is reached in 160, 100, and 40 min for the samples 10:7, 10:8.5, and 10:10, respectively. To be more quantitative regarding the difference of various samples, the impedance at 10 kHz, a safe frequency for IBC,^[26,73] is reported against dissolution time in Figure 2c.

The circuit model of the exploited IBC coupling mechanism, containing signal generator, pill, body, skin, and receiver, is proposed in Figure 2d. Briefly, in the pill, there is a constant impedance element (the conductive oleogel, Z_C) and a variable impedance one (degradable/digestible drug-filled matrix, Z_V). The other impedances represent the internal body impedance (Z_B) and the skin impedance (Z_S), and they are constant. Decrease of Z_V leads to a “short circuit” of the signal, allowing the switching from a capacitive to a galvanic IBC coupling regime. This produces a reduction in the read-out signal. The passive modulation of the IBC regime has been verified, with the sample 10:7, exploiting both a grounded (an external waveform generator) and floating (a commercial Integrated Circuit – IC) signal generator as transmitters (details in Materials and Methods). The IBC signal amplitude modulation obtained with a signal generator is reported in Figure 2e. In Figure 2f the normalized peak-to-peak (V_{pp}) read-out signals are reported, along with the simulated results. Noteworthy, the IBC coupling switching leads to a 96.5% amplitude signal reduction. In Figure S15 (Supporting Information) the IBC signal modulation obtained with the IC and the simulator is reported. The simulation results are in good agreement with the experimental results, indicating that the proposed equivalent circuit model describes well the experimental system.

2.3. Drug Release Monitoring

The concomitant drug release has been independently evaluated by UV–vis spectrophotometry. The absorbance of metformin at 233 nm^[74,75] has been measured in order to determine the drug release by interpolating a standard calibration curve in a linear concentration (1–14 $\mu\text{g mL}^{-1}$, Figure S16, Supporting Information). Noteworthy, no chemical modification has been carried out on metformin, therefore, the pharmacokinetic and pharmacodynamic after the release are the same as the pristine drug. The drug release has been evaluated for 160 min, as shown in Figure 3a. The increase of the HEC leads to an increase in the total release of the metformin in the SIF. In particular, a release of $53\% \pm 2\%$, $70\% \pm 3\%$, $76\% \pm 1\%$, and $99\% \pm 1\%$ after 160 min has been reached for the samples 10:5, 10:7, 10:8.5, and 10:10, respectively. The mechanism of drug release of the eDi-MoRe drug-filled composite has been proposed in Figure 3b. After the device immersion in SIF, the HEC in contact with the solution starts to absorb water and swell. This mechanism generates cracks that further augment the available surface for liquid contact and trigger further material swelling/dissolution. This process activates a “domino” effect that results in the surface erosion of the material. The more the material is disintegrated, the more drug is exposed to the liquid solution, and the more drug is dissolved (see the dissolution process in Video S1, Supporting Information for the sample 10:7). Thus, the proposed

schematic mechanism links directly the HEC concentrations and drug release. Drug release data were fitted through the Korsmeyer–Peppas model (Equation. (1)) to evaluate the drug release mechanism:

$$\frac{M_t}{M_\infty} = K \times t^n \quad (1)$$

In this equation, M_t/M_∞ represents the fractional permeated drug for the first 60% of release, t is the time, K is the kinetic constant, and n is the transport exponent.^[76,77] The kinetic constant K provides information on the structural and geometric characteristics of the system (also considered the release velocity constant), whereas n is the exponent of release in the function of time t , which describes the drug release mechanism. In Table 1, the value of K , n , R^2 , and percentage of drug release are reported. The increase of HEC in the composite leads to an increase in the release exponent. The samples 5:10 and 7:10 show a Fickian drug diffusion ($n \leq 0.45$), which means that HEC erosion is slower than the solvent diffusion.^[78] Such behavior is desired for the long-sustained drug release. On the other hand, samples 8.5:10 and 10:10 show an anomalous or non-Fickian diffusion, in which the HEC erosion time becomes comparable to the solvent diffusion.^[78] Therefore HEC plays a key role in regulating both the drug release mechanism (K and n in the table) and the drug bioavailability (drug release % in the table). Indeed, with a low content of HEC, the oleogel hydrophobicity entraps some of the drugs, which remain encapsulated in the oleogel microparticles, resulting in a lower % of drug release.^[58]

A schematic of the pill dissolution, drug release, and wireless passive IBC modulation is reported in Figure 3c. Such a scheme shows the link between these three phenomena, which are strictly related in the eDi-MoRe device and enable the monitoring of pharmacological adherence and real-time drug release. To further prove the link between pill dissolution, drug release and passive IBC modulation, the proof of concept has been validated using the sample with a matrix:HEC ratio of 10:7, which has shown the complete dissolution with a Fickian drug diffusion. Figure 3d displays amplitude signal attenuation read-out obtained with floating signal generator during the drug release at 0, 40, 80, 120, and 160 min and the related metformin release in SIF. At time 0 min, the maximum signal propagation (pure capacitive coupling) is observed and no drug is released. Then with time passing, a reduction of the IBC signal is observed due to the insulating material dissolution and drug release. After ≈ 160 min, the signal reaches its minimum (galvanic coupling), and 72% of the drug has been released in the SIF. The drug release and IBC data have been combined to estimate the passive amplitude signal modulation in relation to the metformin release. In Figure 3e the cumulative drug release and the real-time drug release (time derivative), in relation to the passive IBC (normalized V_{pp} signal) and time, are reported. The direct correlation between the real-time drug release and impedance variation shows an R between 0.7 and 0.9.

The V_{pp} signal vs. drug release curve (Figure 3e) describes the eDi-MoRe device working principle. Such curves have been interpolated with a rational curve ($R^2 = 0.99$, Table S1, Supporting Information) to extract the relation and relevant figures

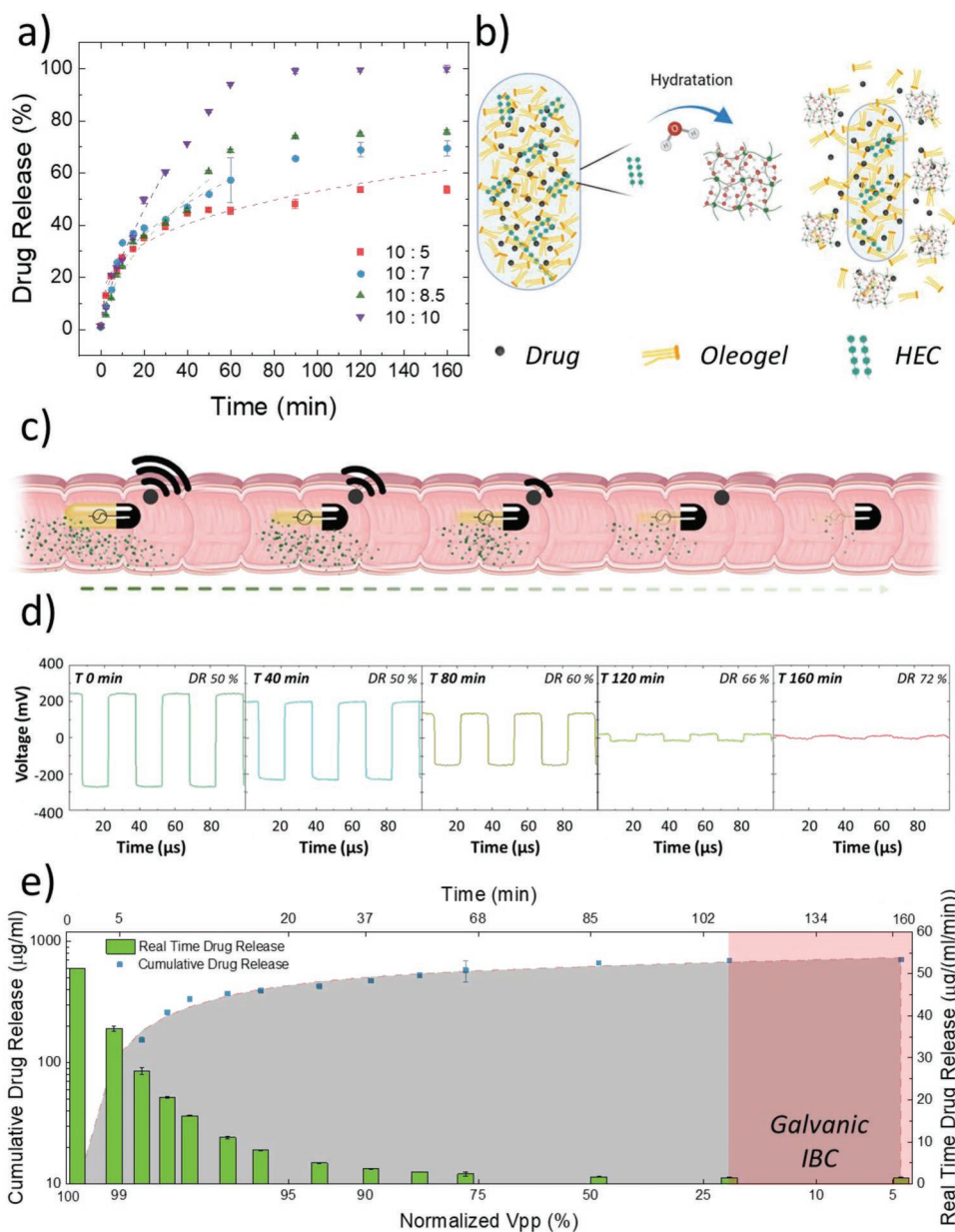


Figure 3. a) Metformin release profiles; b) Schematic of the drug release mechanism for the eDi-MoRe composite; c) Graphic representation of the pill dissolution, drug release, and wireless IBC modulation; d) IBC passive modulation and drug release of 10:7 device in simulated intestinal fluid; e) Device calibration curve, the Vpp axis is reported in Logit scale to highlight the drug release at the start.

Table 1. Parameters of Korsmeyer–Peppas drug release model. K is the kinetic constant, n is the transport exponent, R^2 is the coefficient of determination from the fit, the percentage shows the drug released. The samples are labeled considering the different ratios of oleogel matrix:HEC in the composite.

	10 : 5	10 : 7	10 : 8.5	10 : 10
Drug release [%]	53 \pm 2%	70 \pm 3%	76 \pm 1%	99 \pm 1%
K [s^{-1}]	13	10	6	6
n	0.30	0.42	0.59	0.70
R^2	0.99	0.99	0.98	0.99

of merit of the system. A limit of cumulative drug release detection of $18 \mu\text{g ml}^{-1}$ ($\approx 2\%$ of total drug) and a limit of real-time drug release detection of $2 \mu\text{g mL}^{-1} \text{min}^{-1}$ ($\approx 0.2\%$ of the total drug) have been estimated according to Armbruster et al. with a 95% confidence.^[79,80]

3. Conclusions

A proof-of-principle of an electrically monitored passive drug release system (eDi-MoRe) has been developed from food-grade material and was tested in vitro. When the device comes

in contact with simulated intestinal fluids, a capacitive IBC channel becomes available, and the signal is transmitted, confirming the medication adherence. Then, the dissolution of the drug-filled part of the eDi-MoRe device leads to amplitude modulation of the signal, gradually switching from capacitive to galvanic IBC coupling. Such switching results in a reduction of 96.5% of the read-out signal. A natural hydrophilic polysaccharide (hydroxyethyl cellulose) triggers material disintegration. The amount of hydroxyethyl cellulose affects the whole system by modulating the microstructural properties, erosion process, and total drug release, which ranges from 53% to 99%. The proof of concept device has shown a limit of cumulative drug release detection of $18 \mu\text{g mL}^{-1}$ ($\approx 2\%$ of total drug) and a limit of real-time drug release detection of $2 \mu\text{g mL}^{-1} \text{ min}^{-1}$ ($\approx 0.2\%$ of total drug). Our in vitro results demonstrate that the proposed concept offers an appealing platform for passive drug release that can be electrically monitored in real-time from the ingestion to the complete release. Such results could pave the way to new and long-sought therapy and treatment opportunities, optimizing the therapeutic drug levels and reducing the total drug intake. Further material development will allow a selective and monitored drug release in different parts of the gastrointestinal tract. Moreover, the development of new composite materials will allow the release of hydrophobic drugs by taking advantage of different polymers' solubility in diverse environmental conditions (e.g., hydrogels sensitive to pH, temperature, antigen, and bacteria). The eDi-MoRe concept is compatible with such further developments.

In the future, the integration of an edible signal generator, i.e., an oscillator, and an edible battery, both under development and within the targets of the emerging edible electronics field, will allow in vivo experiments for therapeutic drug monitoring, providing higher personalized medicine being tailored to patients' needs, responses, and risks.

4. Experimental Section

Materials: Beeswax (E 901), Hydroxyethylcellulose (HEC, E1525), NaCl, KH_2PO_4 , NaOH, and HCl were purchased from Sigma–Aldrich. Activated carbon (E153) was purchased from Supelco and morphologically characterized as performed in a previous report.^[55] Sunflower oil was purchased in a local supermarket. Metformin hydrochloride (Mylan) was purchased in the pharmacy. Capsules size 000 gastro-resistant were purchased from Capsugel. Gelatin capsules size 0 were purchased from Your Supplements.

Methods: Conductive oleogel was made following the preparation detailed in the previous work.^[55] Briefly, beeswax and the sunflower oil (25:75 weight ratio) were melt-mixed ($100 \text{ }^\circ\text{C}$ per 20–30 min), then 40 wt% AC was added and mixed for 10 min at the same temperature.

Insulating degradable/digestible matrix was made by melt-mixing 25:75 beeswax sunflower oil ratio ($100 \text{ }^\circ\text{C}$ per 20–30 min). Afterward, the required amount of HEC was added and mixed (10 min – $100 \text{ }^\circ\text{C}$). As the last step, 10% weight of Metformin has been added and mixed (10 min – $100 \text{ }^\circ\text{C}$).

The device processing is graphically described in Figure S2 (Supporting Information). The gelatin pill capsule has been used as a mold for device fabrication through injection molding at the temperature of $100 \text{ }^\circ\text{C}$. The device was extracted from the capsule, wired, and encapsulated in the gastro-resistant capsule prefilled with sunflower oil. Solvents were avoided, and the temperature reached during the production process was $100 \text{ }^\circ\text{C}$, ensuring a green and straightforward

methodology. The described process represents low-cost, large-scale and green manufacturing methods that are compatible with existing pharmaceutical production plants.

The physiological solution consisted of a 0.90 wt% vol of NaCl.

SIF was prepared as described in the United States Pharmacopoeia^[81] and consisted of a solution of 0.05 M KH_2PO_4 adjusted at pH 6.8 with 0.2 molar solution of NaOH without the use of any enzyme.

SGF was prepared as described in the United States Pharmacopoeia^[81] and consisted of a solution of 0.03 M NaCl adjusted at pH 1.2 with 1 M solution of HCl without the use of any enzyme.

Three samples were tested as a minimum for each measurement.

SEM Analysis: SEM measurements were performed using a Tescan MIRA3 operating at an acceleration voltage of 10 kV and recording the secondary electron emission. The samples were prepared as described next. After immersion at $-195.79 \text{ }^\circ\text{C}$ in liquid nitrogen, the samples were cut by tearing them with two tweezers to preserve the original internal morphology and then pretreated by an ultra-thin ($\approx 10 \text{ nm}$) gold sputtering deposition.

Contact Angle Analysis: Static SIF contact angles of the insulating degradable/digestible drug-filled matrix were measured by an optical contact angle device (DataPhysics). Ten microliters of SIF were deposited on the samples.

Dissolution Analysis: The viscosity was measured with a rheometer Malvern Kinexus in a single shear rate 100 s^{-1} with a helix tool configuration. A 45 mL chamber was filled with SIF or SGF and heated at $37 \text{ }^\circ\text{C}$. A metallic sinker with $\approx 500 \text{ mg}$ of material inside was placed on the bottom side of the chamber.

Impedance Analysis: The electrical impedance was measured as described in Figure S8 (Supporting Information) employing a Precision Impedance analyzer Agilent 4294A. The impedance reported in the main manuscript was between points B and C of Figure S8 (Supporting Information). All the measurements were acquired in a range between 100 Hz and 1 MHz.

IBC Characterization: The IBC was measured by connecting terminals A and B to the signal generator and C to an oscilloscope (Tektronix MSO 4054)

Signals generator used:

- 1) Keithley–waveform generator Vpp 500mV – 10 kHz;
- 2) Integrated circuit (IC) Crystal oscillator 3030LC battery powered

Simulations: The simulations were performed exploiting the circuitual model as described in Figure S13 (Supporting Information) and PSpice software. The simulations were performed at 10kHz with a signal of 500mV pk-pk.

Drug release analysis: The drug release was characterized using the same setup employed for the dissolution analysis. One hundred microliters was taken at time point: 2.5, 5, 7.5, 10, 15, 20, 30, 40, 50, 60, 90, 120, and 160 min and replaced with 100 μL of new SIF.

Supporting Information

Supporting Information is available from the Wiley Online Library or from the author.

Acknowledgements

The authors acknowledge the support from the European Research Council (ERC) under the European Union's Horizon 2020 research and innovation program “ELFO”, Grant Agreement 864299. This work also acknowledge funding under the European Union's Horizon 2020 research and innovation program “GREENELIT”, Grant Agreement No. 951747. This work falls within the Sustainability Activity of Istituto Italiano di Tecnologia. The preparation of the specimens for SEM analyses was performed at PoliFab, the micro and nano-technology center of the Politecnico di Milano.

Open access Funding provided by Istituto Italiano di Tecnologia within the CRUI-CARE Agreement.

Conflict of Interest

The authors declare no conflict of interest.

Data Availability Statement

The data that support the findings of this study are available from the corresponding author upon reasonable request.

Keywords

edible electronics, IBC switching, intrabody communication, monitored drug release, oleogel

Received: May 4, 2022

Revised: September 8, 2022

Published online: October 26, 2022

- [1] R. Gossink, J. Souquet, *Advances in Healthcare Technology*, Springer, Berlin **2006**.
- [2] M. Agostini, F. Lunardelli, M. Gagliardi, A. Miranda, L. Lamanna, A. G. Luminare, F. Gambineri, M. Lai, M. Pistello, M. Cecchini, *Adv. Funct. Mater.* **2022**, 2201958.
- [3] J. Kim, A. S. Campbell, B. E.-F. de Ávila, J. Wang, *Nat. Biotechnol.* **2019**, 37, 389.
- [4] L. Piro, L. Lamanna, F. Guido, A. Balena, M. Mariello, F. Rizzi, M. De Vittorio, *Nanomaterials* **2021**, 11, 1479.
- [5] C. Li, C. Guo, V. Fitzpatrick, A. Ibrahim, M. J. Zwierstra, P. Hanna, A. Lechtig, A. Nazarian, S. J. Lin, D. L. Kaplan, *Nat. Rev. Mater.* **2020**, 5, 61.
- [6] C. Steiger, A. Abramson, P. Nadeau, A. P. Chandrakasan, R. Langer, G. Traverso, *Nat. Rev. Mater.* **2019**, 4, 83.
- [7] B. Jacobson, R. S. Mackay, *Lancet* **1957**, 269, 1224.
- [8] M. Mimee, P. Nadeau, A. Hayward, S. Carim, S. Flanagan, L. Jerger, J. Collins, S. McDonnell, R. Swartwout, R. J. Citorik, *Science* **2018**, 360, 915.
- [9] C. J. Bettinger, *Angew. Chem., Int. Ed.* **2018**, 57, 16946.
- [10] C. Dagdeviren, F. Javid, P. Joe, T. von Erlach, T. Bensen, Z. Wei, S. Saxton, C. Cleveland, L. Booth, S. McDonnell, *Nat. Biomed. Eng.* **2017**, 1, 807.
- [11] S. Gerke, T. Minssen, H. Yu, I. G. Cohen, *Nat. Electron.* **2019**, 2, 329.
- [12] K. Kalantar-Zadeh, N. Ha, J. Z. Ou, K. J. Berean, *ACS Sens.* **2017**, 2, 468.
- [13] A. S. Cheifetz, A. A. Kornbluth, P. Legnani, I. Schmelkin, A. Brown, S. Lichtiger, B. S. Lewis, *Am. J. Gastroenterol.* **2006**, 101, 2218.
- [14] A. S. Sharova, F. Melloni, G. Lanzani, C. J. Bettinger, M. Caironi, *Adv. Mater. Technol.* **2021**, 6, 2000757.
- [15] W. Xu, H. Yang, W. Zeng, T. Houghton, X. Wang, R. Murthy, H. Kim, Y. Lin, M. Mignolet, H. Duan, *Adv. Mater. Technol.* **2017**, 2, 1700181.
- [16] G. E. Bonacchini, C. Bossio, F. Greco, V. Mattoli, Y. H. Kim, G. Lanzani, M. Caironi, *Adv. Mater.* **2018**, 30, 1706091.
- [17] A. S. Sharova, M. Caironi, *Adv. Mater.* **2021**, 2103183.
- [18] J.-S. Kang, M.-H. Lee, *Korean J. Intern. Med.* **2009**, 24, 1.
- [19] M. P. Claros, C. V. M. Messa, H. A. García-Perdomo, *Oncol. Rev.* **2019**, 13, 1.
- [20] I. Lerman, *Arch. Med. Res.* **2005**, 36, 300.
- [21] B. Jankowska-Polańska, K. Zamęta, I. Uchmanowicz, A. Szymańska-Chabowska, D. Morisky, G. Mazur, *J. Geriatr. Cardiol.* **2018**, 15, 153.
- [22] H. Rosen, T. Aribat, *Nat. Rev. Drug Discov.* **2005**, 4, 381.
- [23] E. Sabaté, E. Sabaté, *Adherence to Long-Term Therapies*, World Health Organization, Geneva **2003**.
- [24] G. Traverso, R. Langer, *Nature* **2015**, 519, S19.
- [25] M. Kleinrock, *IMS Institute for Healthcare Informatics*, Russell Publishing Ltd, Parsippany, NJ **2012**.
- [26] H. Hafezi, T. L. Robertson, G. D. Moon, K.-Y. Au-Yeung, M. J. Zdeblick, G. M. Savage, *IEEE Trans. Biomed. Eng.* **2014**, 62, 99.
- [27] J. F. Van Boven, I. Tsiligianni, I. Potočnjak, J. Mihajlović, A. L. Dima, U. N. Makovec, T. Agh, P. Kardas, C. M. Ghiciuc, G. Petrova, *Front. Pharmacol.* **2021**, 12, 748702.
- [28] I. Ahmed, N. S. Ahmad, S. Ali, S. Ali, A. George, H. S. Danish, E. Uppal, J. Soo, M. H. Mobasheri, D. King, *JMIR mhealth uhealth* **2018**, 6, e6432.
- [29] J. W. Scannell, A. Blanckley, H. Boldon, B. Warrington, *Nat. Rev. Drug Discov.* **2012**, 11, 191.
- [30] H. He, Q. Liang, M. C. Shin, K. Lee, J. Gong, J. Ye, Q. Liu, J. Wang, V. Yang, *Front. Chem. Sci. Eng.* **2013**, 7, 496.
- [31] J. Li, D. J. Mooney, *Nat. Rev. Mater.* **2016**, 1, 1.
- [32] S. Mura, J. Nicolas, P. Couvreur, *Nat. Mater.* **2013**, 12, 991.
- [33] J. A. Hubbell, A. Chilkoti, *Science* **2012**, 337, 303.
- [34] F. Yamashita, M. Hashida, *Adv. Drug Delivery Rev.* **2013**, 65, 139.
- [35] M. Hashida, *Adv. Drug Delivery Rev.* **2020**, 157, 71.
- [36] X. Mu, M. J. Tobyn, J. N. Staniforth, *J. Controlled Release* **2003**, 93, 309.
- [37] K. E. Anderson, *Clin. Pharmacokinet.* **1988**, 14, 325.
- [38] C.-A. Chen, C. Wu, P. A. R. Abu, S.-L. Chen, *Appl. Sci.* **2018**, 8, 1474.
- [39] T. Kawanishi, presented at 2019 *IEEE Globecom Workshops (GC Wkshps)*, XX, Hawaii, USA, December, **2019**.
- [40] T. G. Zimmerman, *IBM Syst. J.* **1996**, 35, 609.
- [41] D. Naranjo-Hernández, A. Callejón-Leblic, Ž. Lučev Vasić, M. Seyedi, Y.-M. Gao, *Wirel Commun Mob Comput* **2018**, 2018.
- [42] J. E. Ferguson, A. D. Redish, *Expert Rev. Med. Devices* **2011**, 8, 427.
- [43] Ž. Lučev, I. Krois, M. Cifrek, *Wearable and Autonomous Biomedical Devices and Systems for Smart Environment*, Springer, Berlin **2010**.
- [44] D. Das, S. Maity, B. Chatterjee, S. Sen, *Sci. Rep.* **2019**, 9, 1.
- [45] Y. Wu, D. Ye, Y. Shan, S. He, Z. Su, J. Liang, J. Zheng, Z. Yang, H. Yang, W. Xu, *Adv. Mater. Technol.* **2020**, 5, 2000100.
- [46] K. Hachisuka, A. Nakata, T. Takeda, K. Shiba, K. Sasaki, H. Hosaka, K. Itao, *Sens. Actuators, A* **2003**, 105, 109.
- [47] A. Alshehab, N. Kobayashi, J. Ruiz, R. Kikuchi, S. Shimamoto, H. Ishibashi, *Telemed. J. e-Health* **2008**, 14, 851.
- [48] F. Wolling, C. D. Huynh, K. Van Laerhoven, presented at 2021 *International Symposium on Wearable Computers*, XX, New York, September **2021**.
- [49] T. Kobayashi, Y. Shimatani, M. Kyoso, presented at 2012 *Annual International Conference of the IEEE Engineering in Medicine and Biology Society*, XX, San Diego August **2012**.
- [50] C. J. Bailey, *Diabetologia* **2017**, 60, 1566.
- [51] K. J. Wadher, R. B. Kakde, M. J. Umekar, *Int. J. Pharm. Invest.* **2011**, 1, 157.
- [52] G. G. Graham, J. Punt, M. Arora, R. O. Day, M. P. Doogue, J. Duong, T. J. Furlong, J. R. Greenfield, L. C. Greenup, C. M. Kirkpatrick, *Clin. Pharmacokinet.* **2011**, 50, 81.
- [53] P. H. Marathe, Y. Wen, J. Norton, D. S. Greene, R. H. Barbhayia, I. R. Wilding, *Br. J. Clin. Pharmacol.* **2000**, 50, 325.
- [54] A. S. Sharova, M. Caironi, *Adv. Mater.* **2021**, 33, 2103183.
- [55] P. Cataldi, L. Lamanna, C. Bertei, F. Arena, P. Rossi, M. Liu, F. Di Fonzo, D. G. Papageorgiou, A. Luzio, M. Caironi, *Adv. Funct. Mater.* **2022**, 32, 2113417.
- [56] N. Šegatin, T. Pajk Žontar, N. Poklar Ulrih, *Foods* **2020**, 9, 900.
- [57] S. P. Chakraborty, T. Shanto, A. Murali, S. K. Sikha, N. Paul, J. Andrews, V. Joseph, presented at 2016 *IEEE MTT-S International Microwave and RF Conference (IMaRC)*, XX, New Delhi December **2016**.

- [58] R. Macoon, M. Robey, A. Chauhan, *Eur. J. Pharm. Sci.* **2020**, *152*, 105413.
- [59] R. Macoon, T. Guerriero, A. Chauhan, *J. Colloid Interface Sci.* **2019**, *555*, 331.
- [60] R. Y. Lochhead, *Polymeric Delivery of Therapeutics*, ACS, Washington **2010**.
- [61] L. Lamanna, F. Rizzi, C. Demitri, M. Pisanello, E. Scarpa, A. Qualtieri, A. Sannino, M. De Vittorio, *Cellulose* **2018**, *25*, 4331.
- [62] C. Demitri, L. Lamanna, E. De Benedetto, F. Damiano, M. S. Cappello, L. Siculella, A. Sannino, *Mater. Sci. Eng. C* **2017**, *77*, 548.
- [63] C. Lerk, M. Lagas, J. Fell, P. Nauta, *J. Pharm. Sci.* **1978**, *67*, 935.
- [64] M. Malmsten, B. Lindman, K. Holmberg, C. Brink, *Langmuir* **1991**, *7*, 2412.
- [65] R. Sauerheber, B. Heinz, *Chem. Sci. J.* **2015**, *6*, 109.
- [66] A. Hirata, Y. Takano, Y. Kamimura, O. Fujiwara, *Phys. Med. Biol.* **2010**, *55*, N243.
- [67] M. Li, Y. Song, G. Wang, Q. Hao, K. Zang, presented at 2016 10th International Conference on Sensing Technology (ICST), XX, Nanjing November, **2016**.
- [68] K. Zhang, Q. Hao, Y. Song, J. Wang, R. Huang, Y. Liu, *Sensors* **2014**, *14*, 1740.
- [69] A. M. Aitzaz, J. Kim, T. Kim, K. D. Park, S. Cho, *Appl. Sci.* **2019**, *9*, 4049.
- [70] C. Gabriel, S. Gabriel, Y. E. Corthout, *Phys. Med. Biol.* **1996**, *41*, 2231.
- [71] Z. A. Deneris, D. E. Pe'a, C. M. Furse, *IEEE J. Electromagn. RF Microw. Med. Biol.* **2019**, *3*, 171.
- [72] N. Sekkat, Y. N. Kalia, R. H. Guy, *J. Pharm. Sci.* **2002**, *91*, 2376.
- [73] M. S. Wegmueller, M. Oberle, N. Felber, N. Kuster, W. Fichtner, *IEEE Trans. Instrum. Meas.* **2009**, *59*, 963.
- [74] L.-D. Hu, Y. Liu, X. Tang, Q. Zhang, *Eur. J. Pharm. Biopharm.* **2006**, *64*, 185.
- [75] A. V. Stuart, Y. Clement, P. Sealy, R. Löbenberg, L. Montane-Jaime, R. Maharaj, A. Maxwell, *Dissolution Technol.* **2015**, *22*, 17.
- [76] M. L. Bruschi, *Strategies to Modify the Drug Release from Pharmaceutical Systems*, Woodhead Publishing, Sawston, Cambridge **2015**.
- [77] I. Y. Wu, S. Bala, N. Škalko-Basnet, M. P. Di Cagno, *Eur. J. Pharm. Sci.* **2019**, *138*, 105026.
- [78] Y. Fu, W. J. Kao, *Expert Opin. Drug Delivery* **2010**, *7*, 429.
- [79] D. A. Armbruster, T. Pry, *Clin. Biochem. Rev.* **2008**, *29*, S49.
- [80] L. Lamanna, F. Rizzi, V. R. Bhethanabotla, M. De Vittorio, *Biosens. Bioelectron.* **2020**, 112164.
- [81] S. G. Fluid, T. In, *Natl. Formul.* **2000**, *9*.